We are IntechOpen,
the world's leading publisher of Open Access books
Built by scientists, for scientists

6,900
Open access books available

185,000
International authors and editors

200M
Downloads

154
Countries delivered to

Our authors are among the

TOP 1%
most cited scientists

12.2%
Contributors from top 500 universities

CLARIVATE ANALYTICS

BOOK CITATION INDEX

INDEXED

WEB OF SCIENCE™

Selection of our books indexed in the Book Citation Index
in Web of Science™ Core Collection (BKCI)

Interested in publishing with us?
Contact book.department@intechopen.com

Numbers displayed above are based on latest data collected.
For more information visit www.intechopen.com

Five-Wheeled Wheelchair with an Add-On Mechanism and Its Semiautomatic Step-Climbing and -Descending Function

Masayoshi Wada and Yu Munakata

Abstract

In this chapter, we propose a novel add-on electric drive system for propelling a manual wheelchair on the floor together with an advanced function to climb and descend a step with no human support. The proposed add-on mechanism consists of an active-caster drive wheel and a reconfigurable link mechanism with a linear actuator to change the location of the drive wheel relative to a wheelchair. By attaching the mechanism to a manual wheelchair, we build a five-wheeled wheelchair. Since the drive wheel is attached on the back of the wheelchair, a risk of falling to the back is significantly reduced. To surmount a step with no help, we develop a step-climbing and -descending strategy by using the proposed wheelchair with a reconfigurable link mechanism. The five-wheel configuration guarantees a static stability of the wheelchair when some wheels are hovered from the ground. The function is used in step-climbing and -descending strategies to realize the transfer of a wheelchair user. In order to reduce the effort of a wheelchair user to control the complicated step surmount strategies, semiautomatic system is installed on the prototype wheelchair whose availability is verified through experiments.

Keywords: active-caster, wheelchair add-on electric drive, step-climbing and -descending, semiautomatic control

1. Introduction

For the aging society worldwide, need for machines that can support human moving capabilities gets more and more importance in recent years. Electric wheelchairs [1] are one of the most popular solutions for overcoming the aging problem in the past few decades. Electric-powered wheelchairs are used as one of the moving support devices not only for injured

people but also for the elderly. Among the electric-driven wheelchairs, a "motorized wheelchair" has become popular in recent years. Different from a standard electric wheelchair, which is designed as electric-driven, a motorized wheelchair is composed of a manual wheelchair frame and an add-on electric drive module. Because it is foldable and light weight, users may carry it by cars to travel long distances easily.

A pair of electric drive modules for propelling left and right large wheels of a manual wheelchair are popular and commercially available (**Figure 1(a)**) [2]. Since the main parts are from a manual wheelchair, the diameter of a front caster is quite small, which prevents a motorized wheelchair from passing over a few centimeters step. Addition to this, if drive motors on the left and right provides large torque when the front casters stack into the gap or step, a wheelchair might fall in back since the reaction torques of the drive motors are applied to the wheelchair frame. In contrast, a five-wheeled wheelchair composed of a manual wheelchair and a single-wheel drive system was proposed (**Figure 1(b)**) [3]. The installed drive wheel is a standard orientable wheel, which can change its orientation at a steady point on the ground. This type of wheel has a nonholonomic constraint in its sideways direction and cannot control two degrees of freedom (2DOF) motion independently.

Toward the problem of step-climbing and -descending of wheelchairs, a lot of systems and mechanisms have been conducted. Wheelchairs with additional legs [4], some spoke wheels [5, 6], step-climbing method by the dynamic control as the inverted pendulum [7, 8], triangle frame with three wheels at the triangle vertices [9–11], and tracks on each side [12] have been proposed. The iBot wheelchair [13], which has the dynamic balancing functionality as an inverted pendulum, and Scaleve [14], which has additional tracks to climb over steps, have also been introduced. However, they are too heavy to carry them by personal cars.

A step-climbing method of the front casters with steering shafts fixed by the special mechanism [15], and a step-climbing and -descending strategies with a partner robot [16] are proposed to enhance the step-climbing capability of a manual wheelchair. The former is the step-climbing method only for the front casters and step-descending method has not been reported. The real-world applications of the latter system are quite limited.

In this paper, we propose an add-on mechanism to satisfy the step-climbing and -descending strategies, and in the both the strategies, the wheelchair approaches a step from the front. In our previous works, we proposed a five-wheeled wheelchair equipped with an add-on mechanism on the back of a manual wheelchair [17]. The add-on mechanism is composed of an active-caster, a linear actuator, and some link frames, which is connected to a manual
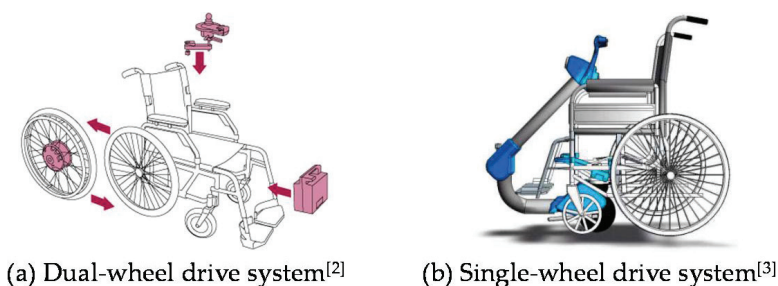

(a) Dual-wheel drive system[2]   (b) Single-wheel drive system[3]

Figure 1. Conventional motorized wheelchair. (a) Dual-wheel drive system [2]. (b) Single-wheel drive system [3].

wheelchair frame. The active-caster [18] is used as a propelling mechanism for the manual wheelchair. The linear actuator is used as the wheelchair's posture change mechanism. In the climbing process of the front casters, they can be hovered from the ground by changing the location of the active-caster to backward of the wheelchair using the linear actuator. The large wheels and the drive wheel can be hovered from the ground, and pass over a step using the same method as that in the front casters. In the descending motion, the large wheels of the wheelchair can be landed on the ground by applying the hovering motion of the front casters to avoid the wheelchair frame from leaning forward. We derive the mechanical design condition for satisfying the static stability during the proposed step-climbing and -descending strategy. We determine the link configuration parameters of the add-on mechanism based on the derived mechanical condition and that of the step-climbing strategy. The descending abilities are realized together with the step-climbing function by constructing the add-on mechanism prototype. Also, we propose the semiautomatic control system for the proposed step-climbing and -descending strategies. By using the step detecting system, the front casters are hovered from the ground. Moreover, we propose the control method of the add-on mechanism in each process of the step-climbing and -descending motion. We have subsequently confirmed that the user could pass over a step automatically, using the proposed step-climbing and -descending strategies after the prototype assembly.

2. An add-on drive system

2.1. Active-caster

Figure 2 shows a schematic top view of an active-caster and an overview of the drive unit whose wheel axis is located in an offset position of the steering axis as a passive caster. The distance between the axes is called "caster-offset" as indicated by a parameter "s" in the figure.

The active-caster is used as a drive wheel by actuating a wheel shaft and a steering shaft by respective motors. To provide a traction power in an arbitrary direction with an arbitrary magnitude, a wheel rotation and a steering rotation are coordinated by a control law represented in Eq. (1). The equation includes cosine and sine functions of wheel orientation θ to derive the wheel and steering rotations, ω_w and ω_s. The wheel angle θ is measured by an absolute angle sensor and drive wheel, and steering axes are driven by the independent motors in appropriate ratios of angle θ, as represented in Eq. (1).
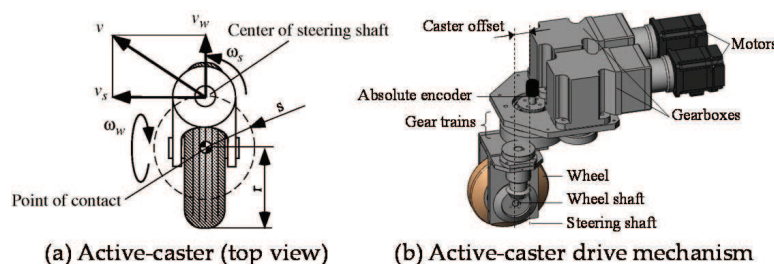

Figure 2. Active-caster. (a) Active-caster (top view). (b) Active-caster drive mechanism.

$$\begin{bmatrix} \omega_w \\ \omega_s \end{bmatrix} = \begin{bmatrix} \dfrac{\cos\theta}{r} & 0 \\ 0 & \dfrac{\sin\theta}{s} \end{bmatrix} v \tag{1}$$

where, θ: angle between the velocity vector and wheel,

r: wheel radius,

s: caster offset,

ω_w: rotation of wheel axis,

ω_s: rotation of steering axis, and

v: required velocity vector on the steering shaft.

The active-caster was developed for holonomic and omnidirectional mobile robots by installing two or more numbers of active-caster units on a robotic platform [19]. However, one active-caster unit is used for the electric drive system for propelling the five-wheeled wheelchair whose top view is shown in **Figure 3**. The active-caster generates 2DOF velocity vector whose components are represented by v_s and v_w as shown in **Figure 2(a)**. These components are generated independently by a coordinated control, 2DOF of the wheelchair frame, which can be controlled independently as well. The relationships of the wheelchair motion and the active-caster velocity components are represented in Eq. (2), where x_p is a location of the active-caster steering shaft relative to the midpoint of large wheels of the manual wheelchair as shown in **Figure 3**. From Eqs. (1) and (2), we can derive a control law of the proposed five-wheeled wheelchair as in Eq. (3) to control it in the same manner as a standard electric wheelchair using a joystick.
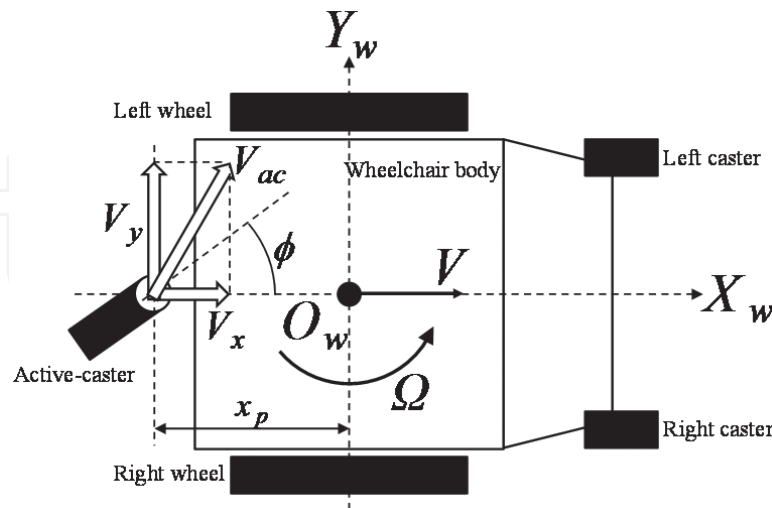

Figure 3. Five-wheeled wheelchair with an add-on active-caster drive wheel.

$$\begin{bmatrix} V_x \\ V_y \end{bmatrix} = \begin{bmatrix} 1 & 0 \\ 0 & x_p \end{bmatrix} \begin{bmatrix} V \\ \Omega \end{bmatrix} \tag{2}$$

$$\begin{bmatrix} \omega_w \\ \omega_s \end{bmatrix} = \begin{bmatrix} \dfrac{\cos\phi}{r} & \dfrac{x_p \sin\phi}{r} \\ \dfrac{-\sin\phi}{s} & \dfrac{x_p \cos\phi}{s} \end{bmatrix} \begin{bmatrix} V \\ \Omega \end{bmatrix} \tag{3}$$

where V is a translation velocity and Ω is an angular velocity of a wheelchair frame while ϕ is an orientation of the active-caster relative to the wheelchair frame.

2.2. A reconfigurable link mechanism

A five-wheeled wheelchair is composed of a manual wheelchair and the active-caster drive unit. To connect these, we develop a reconfigurable link mechanism to change the location of the active-caster depending on its environments. The major purpose of installing the link mechanism is to surmount a step with no support of caregivers. To vary the location and the height of the active-caster relative to a wheelchair frame, we design a link mechanism whose configuration can be varied by a linear actuator. **Figure 4(a)** shows a schematic side view of the link mechanism with a wheelchair frame and the active-caster. The link mechanism includes three links AB, AC, and BD. The active-caster is installed at point C and touches to the ground. Those links are connected by pin joints at point A, B, and D. The links AC and BD are made of aluminum bars with constant lengths while link AB is composed by cylinder of a linear actuator whose length can be varied by motor actuation. As the length of AB changes, the overall link configuration changes, which results in the change of the location of the active-caster. As the linear actuator extends as shown in **Figure 4(b)**, the active-caster moves backward and the active-caster gets closer to the wheelchair and simultaneously pushes the ground when the linear actuator shrinks as in **Figure 4(c)**.
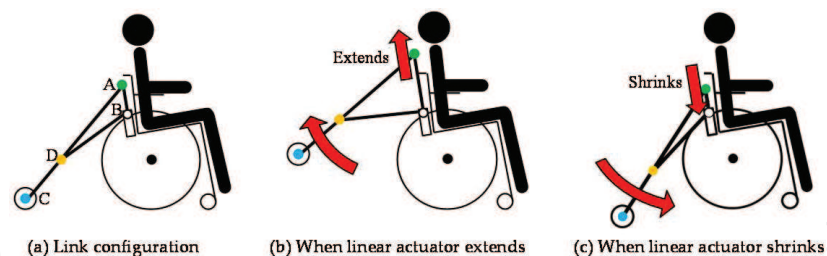

(a) Link configuration   (b) When linear actuator extends   (c) When linear actuator shrinks

Figure 4. A reconfigurable link mechanism and its motions. (a) Link configuration. (b) When linear actuator extends. (c) When linear actuator shrinks.

3. Step-climbing and -descending strategies for five-wheeled wheelchair

3.1. Step-climbing strategy

The series of motions performed by the wheelchair is shown in **Figure 5**. First, the wheelchair stops in front of the step (**Figure 5(a)**). Next, the wheelchair performs a static wheelie motion and the front casters are hovered from the ground (**Figure 5(b)**). Then, the wheelchair moves forward by maintaining the static wheelie and the front casters reaches on the top of the
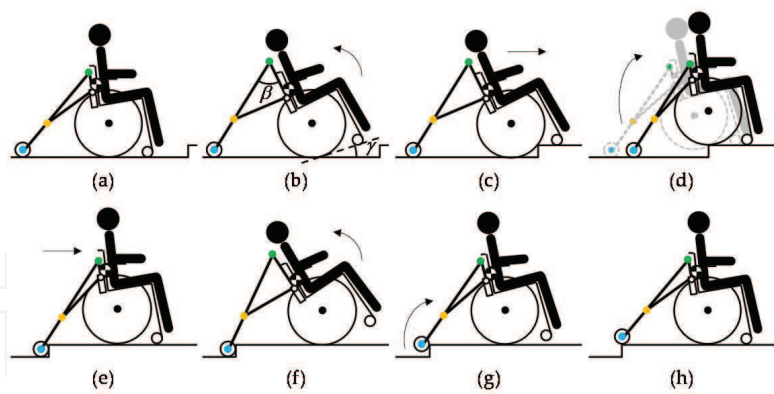
Figure 5. A step-climbing strategy for a five-wheeled wheelchair.

step (**Figure 5(c)**). Note that the center of gravity locates in the area defined by the two large wheels and the drive wheel; therefore, a wheelchair user can move forward with maintaining the posture of the static wheelie without a balancing control. After the front casters climbing, the large wheels are lifted by pushing down the active-caster to the ground (**Figure 5(d)**). By the forward motion, the large wheels pass over the step (**Figure 5(e)**). After the large wheels climbing, the wheelchair performs a static wheelie motion on the step (**Figure 5(f)**). After the completion of the static wheelie, large wheels are locked by the braking mechanism of the wheelchair. By coordinated motions of the drive wheel and the linear actuator (**Figure 5(g)**), the drive wheel climbs up the wall of a step and reaches to the top. Thus, a series of step-climbing sequence is completed (**Figure 5(h)**).

3.2. Step-descending strategy

We then explain the step-descending strategy in which a user approaches a step from the front side of the wheelchair. To avoid a risk of falling from the top of a step to the ground, we apply the static wheelie motion in the step-descending process as well. **Figure 6** shows the series of motions for the step-descending process. First, the wheelchair stops in front of the step (**Figure 6(a)**). Next, the wheelchair performs a static wheelie to hover the front casters and
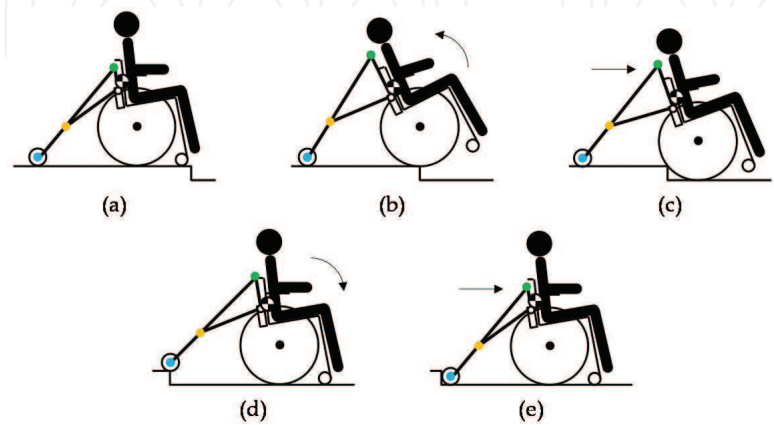

Figure 6. A step-descending strategy for a five-wheeled wheelchair.

moves to the edge of the step (**Figure 6(b)**). After applying gentle brake to the large wheels of a wheelchair for reducing an impact of landing on the ground, the wheelchair starts to descend a step by maintaining the static wheelie situation (**Figure 6(c)**). The breaks are unlocked after the large wheel lands on the ground, the front casters can then be landed on the ground using the linear actuator motion (**Figure 6(d)**). The drive wheel lands on the ground after the forward movement of the wheelchair (**Figure 6(e)**). Thus, the step-descending motion of the wheelchair is completed.

4. Design of a reconfigurable link mechanism

4.1. Geometry model of the reconfigurable link mechanism

In this section, we derive a geometry model of the proposed link mechanism. **Figure 7** shows a schematic side view of the reconfigurable link mechanism with a manual wheelchair. We define a coordinate system of the wheelchair Σ-$X_w Z_w$, where the origin of the coordinate is at the point of contact between the large wheel and the ground as shown in **Figure 7**. The linear actuator on the link mechanism is attached at the back of the wheelchair frame at an angle α. Other links are connected to the linear actuator body, point B, and a top of the cylinder, point A. Coordinates of points A, C, and D are derived as the relative position from point B.

$$\begin{bmatrix} x_a \\ z_a \end{bmatrix} = \begin{bmatrix} \cos\alpha & -\sin\alpha \\ \sin\alpha & \cos\alpha \end{bmatrix} \begin{bmatrix} 0 \\ u_L \end{bmatrix} + \begin{bmatrix} x_b \\ z_b \end{bmatrix} \tag{4}$$

$$\begin{bmatrix} x_c \\ z_c \end{bmatrix} = \begin{bmatrix} \cos\alpha & -\sin\alpha \\ \sin\alpha & \cos\alpha \end{bmatrix} \begin{bmatrix} -l_0\sin\beta \\ u_L - l_0\cos\beta \end{bmatrix} + \begin{bmatrix} x_b \\ z_b \end{bmatrix} \tag{5}$$

$$\begin{bmatrix} x_d \\ z_d \end{bmatrix} = \begin{bmatrix} \cos\alpha & -\sin\alpha \\ \sin\alpha & \cos\alpha \end{bmatrix} \begin{bmatrix} -l_1\sin\beta \\ u_L - l_1\cos\beta \end{bmatrix} + \begin{bmatrix} x_b \\ z_b \end{bmatrix} \tag{6}$$

Here, u_L is the length of the link AB, which can be varied by the motion of the linear actuator, $l_{\{0, 1, 2\}}$ are the lengths of the links AC, AD, and BD, $x_{\{a, b, c, d\}}$ and $z_{\{a, b, c, d\}}$ are the coordinates of
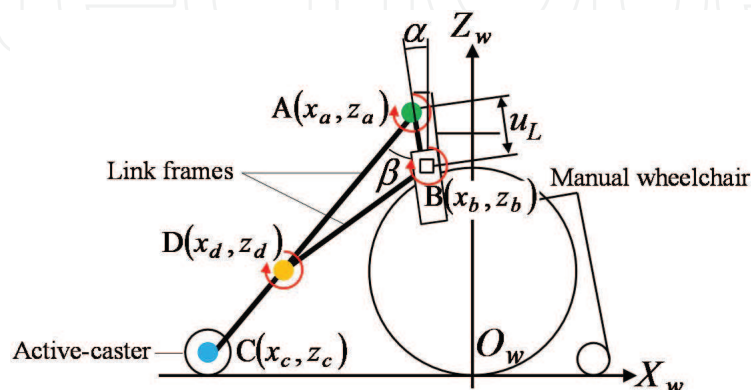

Figure 7. Geometry of a reconfigurable link mechanism.

the points A, B, C, and D along Σ-$X_w Z_w$ axis, respectively. The constant angle α is the inclination of the linear actuator relative to the vertical axis Z_w and β is a variable angle between the link AD and the link AB ($\angle$BAD). We will derive geometric conditions of the link lengths of the mechanism to realize the proposed step-climbing and -descending strategies for the five-wheeled wheelchair.

4.2. Design conditions for climbing up a 100 mm step

Now, we set our target of the surmountable maximum step height to 100 mm, under the assumption that a 100 mm step-climbing capability might allow disable persons to extend their activity in public spots including transfer to trains, passing over steps and gaps in outdoor environments.

At first, we confirm design conditions about the step-climbing of the front casters. In the proposed step-climbing method, the front casters must be hovered 100 mm off the ground for the static wheelie motion. In this motion, the wheelchair frame inclines to the backside. To realize the motion, the link mechanism changes the shape as shown in **Figure 8(a)** in which the active-caster moves backward. The inclination of the wheelchair γ for climbing over a 100 mm high step is represented by the following equation:

$$\gamma = \tan^{-1}\left(\frac{h}{l_f}\right) = 16(\text{deg}) \tag{7}$$

where, h is the height of the step, and l_f is the length between the large wheels and front casters.

Secondly, we confirm the designing condition about the step-climbing of the large wheels. In the proposed method, the large wheels must be hovered 100 mm from the ground. For hovering the motion of the large wheels, the linear actuator changes the height of the drive wheel to locate at 100 mm lower than the ground level as shown in **Figure 8(b)**.

4.3. Design conditions for descending a 100 mm step

Figure 9 shows a schematic view of the wheelchair at a transient moment in which the large wheels descend a step. To prevent wheelchair to fall in the forward direction, a required
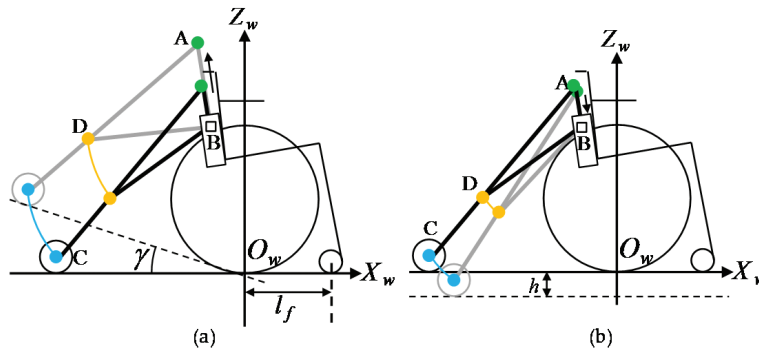

(a)   (b)

Figure 8. Configurations of a link mechanism. (a) Configuration for static wheelie. (b) Configuration for large wheel hovering.
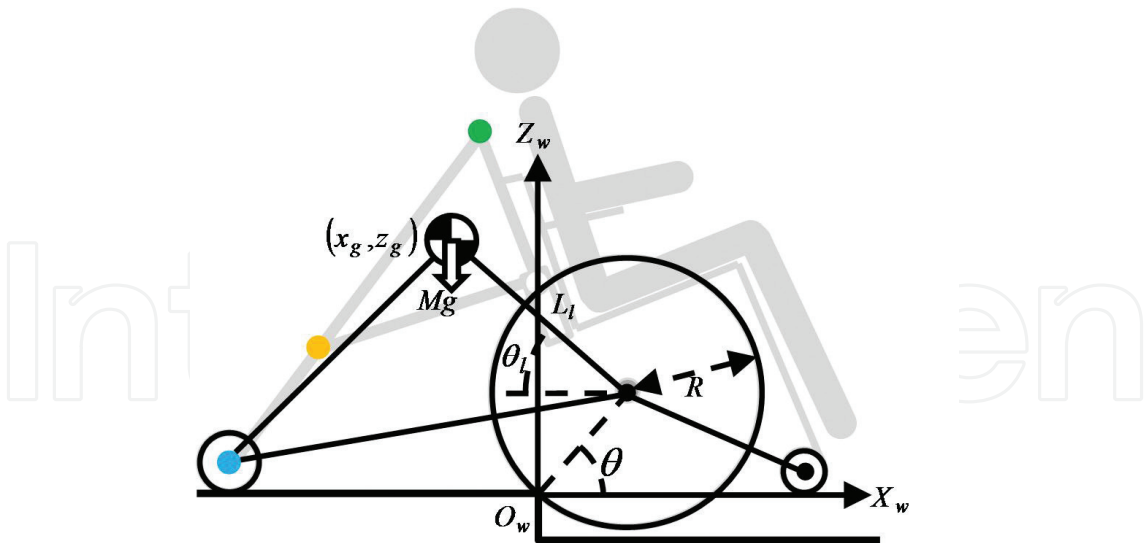
Figure 9. Step-descending model of a five-wheeled wheelchair.

condition for the wheelchair is to maintain the center of gravity not to go beyond the step edge. The condition is represented by a coordinate of the wheelchair along X-axis, x_g as,

$$x_g = R \cos\theta - L_l \cos\theta_l \leq 0 \qquad (8)$$

where, R is a radius of the large wheel, L_l is the length between the drive wheel and the center of gravity, and θ_l is the angle between the line L_l and the X_w axis as shown in **Figure 9**.

4.4. Design of the link mechanism

To satisfy the conditions derived above, we determined the parameters of link mechanism for a prototype wheelchair as shown in **Table 1**.

	Symbol	Value	Unit
Length of the links	l_{AC}	0.91	m
	l_{AD}	0.60	m
	l_{BD}	0.51	m
Attachment position	α	8.0	deg
	x_b	−0.13	m
	z_b	0.60	m
Center of gravity (stand condition)	M	124.6	kg
	x_g	−0.054	m
	z_g	0.50	m
Center of gravity (wheelie motion)	x_g	−0.13	m
	z_g	0.62	m

Table 1. Parameters of the prototype wheelchair and the link mechanism.
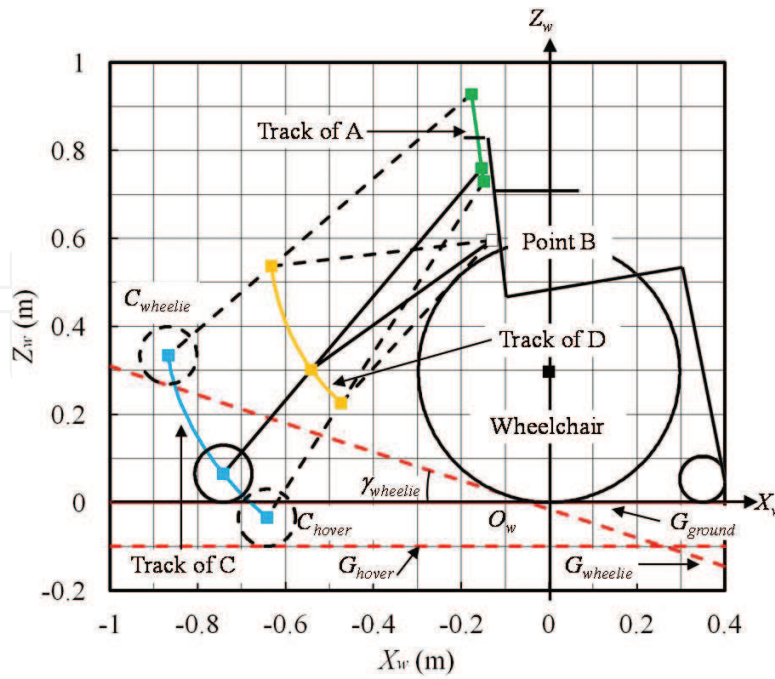
Figure 10. Calculated trajectory of the link mechanism.

By using these parameters, we calculated the motion of the link mechanism. According to the change in the length of link AB, we plotted the trajectories of the points A, C, and D of the proposed mechanism by using Eqs. (4)–(6).

The result is shown in **Figure 10**. As the linear actuator stretches, the drive wheel moves to the back of the wheelchair, by which the inclination γ satisfies the requirement for the static wheelie. Hence as the linear actuator shrinks, the drive wheel gets closer to the wheelchair and pushes the ground for hovering the large wheels to reach a 0.1m high.

5. Semiautomatic control system for step-surmounting motion

In this study, we use laser range finder (LRF) to measure the height of the step and the distance between the wheelchair and the step as shown in **Figure 11(a)**. The measurement result of the step by LRF is shown in **Figure 11(b)**. In **Figure 11(b)**, the positions (i)–(iv) are shown
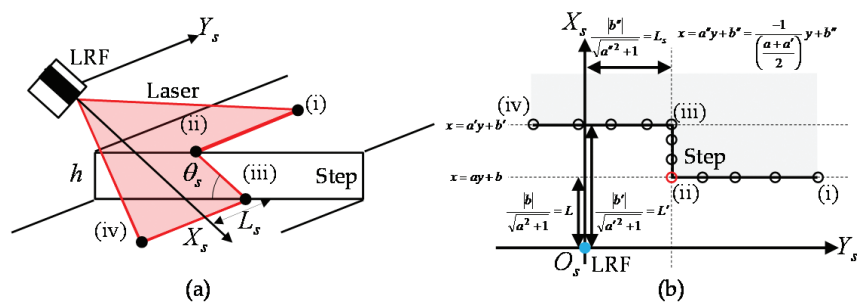

Figure 11. Measurement of the step height and the distance by LRF.

as corresponding to **Figure 11(a)**. The each measurement point by LRF has the coordinates, x and y, on the coordinates system at the center of LRF.

From the LRF data, three lines are identified: the first one represents the top surface of a step, the second one represents the ground, and the last one represents the wall of a step. Those lines are represented as:

$$x = ay + b : \text{step surface}$$
$$x = a'y + b' : \text{ground}$$
$$x = a''y + b'' : \text{step wall}$$

(9)

By using constants in these equations, the height of the step, h, and the distance between LRF and the step, L_s, are derived by the following equations:

$$L_s = \frac{|b''|}{\sqrt{a''^2 + 1}}$$

(10)

$$h = (L' - L)\sin\theta_s = \left(\frac{|b'|}{\sqrt{a'^2 + 1}} - \frac{|b|}{\sqrt{a^2 + 1}}\right)\sin\theta_s$$

(11)

where L and L' are the distances from LRF sensor to a step surface and the ground, respectively. An angle θ_s represents an inclination of a laser scan surface and the ground which can be known as a constant.

By using the measured height of the step h, and the distance to the step L_s, the static wheelie motion and translation motion of the wheelchair can be performed simultaneously to minimize the time for approaching to a step. Moreover, coordinated controls of the linear actuator and the active-caster can be realized for maintaining certain contacts between the large wheels and a step edge for climbing the large wheels.

6. Prototyping

The prototype wheelchair was designed and built whose 3-dimensional Computer Aided Design (3D CAD) models are shown in **Figure 12**. The add-on mechanism, which includes the active-caster and the reconfigurable link mechanism with a linear actuator, is attached on the back of a frame of a manual wheelchair. The stroke of the linear actuator is 200 mm and the maximum power is 144 W. To drive the active-caster, two motors are installed, whose capacities are 200 W each. The diameter of the drive wheel is 130 mm with 45 mm caster offset. Two sensors (LRF) are attached on the side of the wheelchair frame to measure the step whose locations are illustrated in **Figure 13**.

For maneuvering the wheelchair around normal environments, a user can operate the wheelchair by using a joystick on an arm rest as same as in the standard electric wheelchair.

To surmount a step, a user gives a command to a PC (which is not shown in the Figures) to launch the semiautomatic program, which controls the step surmount strategies based on the measured step height and the distance detected by LRFs.
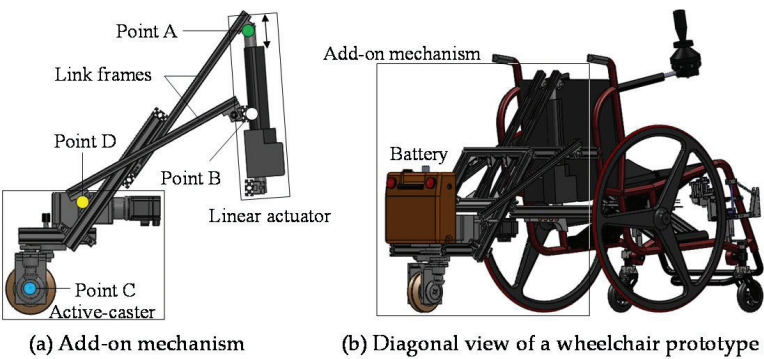
(a) Add-on mechanism   (b) Diagonal view of a wheelchair prototype

Figure 12. Prototype of a five-wheeled wheelchair with an add-on mechanism. (a) Add-on mechanism. (b) Diagonal view of a wheelchair prototype.
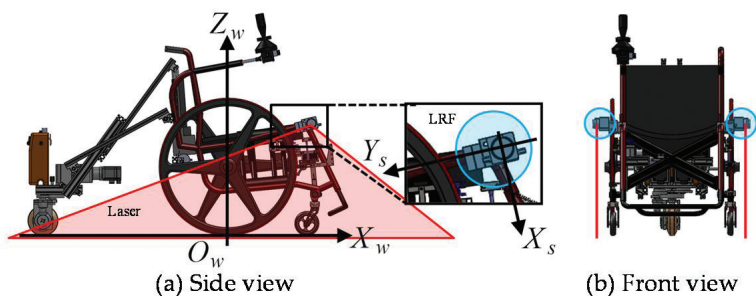

(a) Side view   (b) Front view

Figure 13. Laser sensors for semiautomatic system. (a) Side view. (b) Front view.

7. Experiment

We propose an add-on electric drive system with a reconfigurable link mechanism for a manual wheelchair. We also propose a semiautomatic system for reducing the user effort to operate a wheelchair to surmount a step. To verify the availability of the prototype wheelchair with the semiautomatic system, we tested the step-climbing and -descending processes of the wheelchair using the prototype. In the experiment, we tested the step-climbing and -descending of a 100 mm step.

7.1. Step climbing

The experimental results are shown in **Figure 14**. In **Figure 14(a)–(h)**, each snapshot of the wheelchair corresponds to **Figure 5(a)–(h)**. The experiments were performed by using the semiautomatic operating system. First, the wheelchair is stopped in front of the step by the user operation using joystick (**Figure 14(a)**). After the user commanded to start the semiautomatic operation, LRFs measured the step height and the distance to the step. Then, the wheelchair approached to the step by performing a static wheelie motion with hovering the front casters not to collide with a step (**Figure 14(b)**). After the large wheels contact the step edge, the wheelchair climbed the step by pushing the active-caster down the ground to lift up the large wheels with maintaining the contacts between the large wheels and the step

edge (**Figure 14(c)–(e)**). After the climbing of the large wheels, the static wheelie motion was performed on the top of the step (**Figure 14(f)**). The brake mechanism was then activated after the completion of the static wheelie, for preventing the large wheel to rotate for the drive wheel climbing process. Then the linear actuator changed the link mechanism to locate the drive wheel closer to the wheelchair frame to provide an enough load to the step wall. Together with the linear actuator movements, the drive wheel rotated for climbing the step
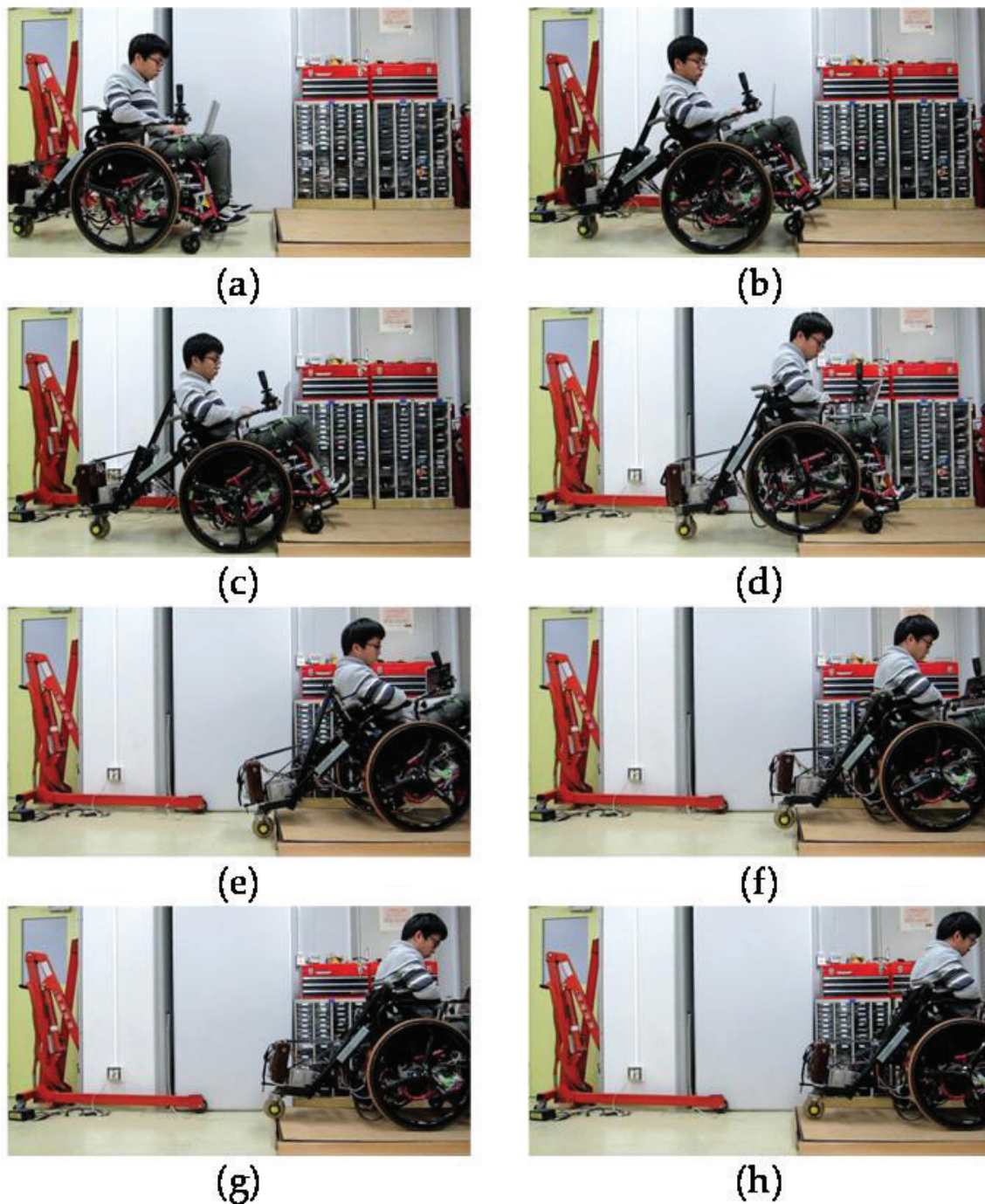

Figure 14. Semiautomatic assist system (step-climbing strategy).

wall (**Figure 14(g)**). Even though the step height was much higher than the diameter of the drive wheel, the drive wheel was successfully able to climb up the step wall since enough load was applied to the step wall by the linear actuator. By unlocking the brake for the large wheels, the step-climbing process was completed (**Figure 14(h)**). From the above all, we confirmed that the wheelchair could climb over a step by the semiautomatic system.

7.2. Step descending

Figure 15 shows the experimental results of the step-descending motion with the semi-automatic operation system. First, the wheelchair stopped in front of the step by the user operation using joystick (**Figure 15(a)**). After the user commanded to start the semiautomatic motion, LRFs measured the step height and the distance between the step edge and the wheelchair. Then, the wheelchair approached to the step by performing a static wheelie motion and stopped to locate the point of contact of the large wheels on the edge of the step (**Figure 15(b)**). After the gentle brakes of the large wheels were activated, the wheelchair descended the step by propelling the drive wheel, which made the large wheels to get down the ground (**Figure 15(c)**). Since the wheelchair performed a static wheelie during the step-descending motion, the user could avoid leaning in the forward direction. After large wheels descending motion, the drive wheel approached to the step edge by contacting the front casters to the ground (**Figure 15(d)**). Finally, the drive wheel reached the ground by decreasing the speed of the drive wheel (**Figure 15(e)**).

In this experiment, the wheelchair was able to descend the step by approaching from the front side of a wheelchair. Thus, by the proposed strategy, we realized the step-descending motion with a reduction of a mental burden.
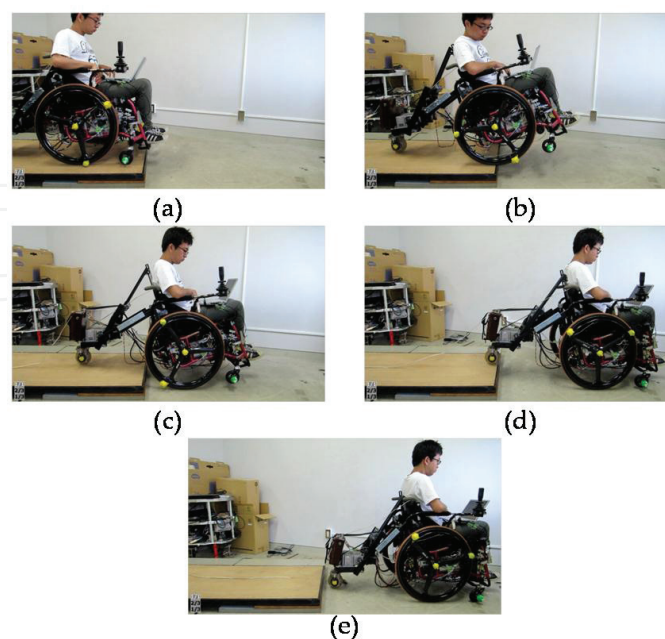

Figure 15. Semiautomatic assist system (step-descending strategy).

8. Conclusion

In this study, we developed a novel add-on mechanism with a reconfigurable link mechanism for a manual wheelchair and realized the step-climbing and -descending strategies. In the climbing motion of the front casters, we proposed the static wheelie motion, in which the large wheels and the drive wheel maintain the static stability with the three-point contact with the ground while the front casters hover from the ground. In the other situation, the large wheels were hovered from the ground by pushing the drive wheel down to the ground using the link mechanism with the linear actuator. We also proposed the climbing motion of the drive wheel by controlling the drive wheel and the linear actuator.

We also proposed the step-descending strategy for approaching a step from the front side of a wheelchair. We derived the design condition of the add-on mechanism for satisfying the static stability of the wheelchair during the proposed descending strategy.

We determined the link length and the position of the add-on mechanism from the design conditions derived from geometric studies. We then confirmed to satisfy the design condition for realizing both of the step-climbing and -descending strategies by link trajectory calculations.

We built the prototype based on the analysis and tested the step-climbing and -descending motions. In the experiments, we confirmed that the proposed wheelchair could climb and descend the step using the proposed strategy and mechanism.

Author details

Masayoshi Wada* and Yu Munakata

*Address all correspondence to: mwada@cc.tuat.ac.jp

Tokyo University of Agriculture and Technology, Koganei-shi, Tokyo, Japan

References

[1] Permobil, Motorized wheelchair, http://www.permobilkk.jp/calling.html. (Supporting Online Materials).

[2] Ulrich Alber GmbH, Scalamobil, https://www.alber.de/. (Supporting Online Materials).

[3] D. Lockton, D. Harrison, "Wheelchair Drive," Project Report for Industrial Design Engineering, Department of Design and Systems Engineering, Brunel University, UK, 2014.

[4] V. Krovi, V. Kumar, "Optimal traction control in a wheelchair with legs and wheels," Proceedings of 4th National Applied Mechanisms and Robotics Conference, 1995.

[5] E. Chaichanasiri, T. Puangumpan, "A prototype of a stair-climbing system for a wheelchair," The Second TSME International Conference on Mechanical Engineering, 2011.

[6] K. Sasaki, Y. Eguchi, K. Suzuki, "Step-climbing wheelchair with lever propelled rotary legs," 2015 IEEE/RSJ International Conference on Intelligent Robots and Systems, pp. 6354-6359, 2015.

[7] N.M. Abdul Ghani, M.O. Tokhi, A.N.K. Nasir, S. Ahmad, "Control of a stair climbing wheelchair," International Journal of Robotics and Automation, 1, 4, pp. 203-213, 2012.

[8] Y. Takahashi, N. Ishikawa, T. Hagiwara, "Soft raising and lowering of front wheels for inverse pendulum control wheelchair robot," Proceedings of the 2003 IEEE/RSJ International Conference on Intelligent Robots and Systems, pp. 3618-3623, 2003.

[9] G. Quaglia, W. Franco, M. Nisi, "Evolution of Wheelchair.q, a stair-climbing wheelchair," The 14th IFToMM World Congress, 2015.

[10] L. Fang, T. Lu, W. He, K. Yuan, "Dynamic and tip-over stability analysis of a planetary wheeled stair-climbing wheelchair," Proceedings of 2012 IEEE International Conference on Mechatronics and Automation, pp. 2541-2546, 2012.

[11] A.S. Shriwaskar, S.K. Choudhary, "Synthesis, modeling and simulation of stair climbing mechanism," International Journal of Engineering Research and Technology, 2, 8, pp. 413-419, 2013.

[12] J. Wang, T. Wang, C. Yao, X-F. Li, C-D. Wu, "Study on interactional characteristics of WT wheelchair robot with stairs during stair-climbing process," Applied Mechanics and Materials, 419, pp. 795-800, 2013.

[13] Segway Inc., iBOT, https://msu.edu/~luckie/segway/iBOT/iBOT.html. (Supporting Online Materials).

[14] Scalevo, http://scalevo.ch/. (Supporting Online Materials).

[15] S. Yokota, D. Chugo, H. Hashimoto, K. Kawabata, "Assistive caster unit of wheelchair for step climbing," International Journal of Mechanical Engineering and Automation, 3(2), pp. 38-45, 2013.

[16] H. Ikeda, et al., "Step climbing and descending for a manual wheelchair with a network care robot," The Second International Conference on Intelligent System and Applications, pp. 95-102, 2013.

[17] Y. Munakata, M. Wada, "A novel step climbing strategy for a wheelchair with active-caster add-on mechanism," IEEE/RSJ International Conference on Intelligent Robots and Systems, pp. 6324-6329, 2015.

[18] M. Wada, S. Mori, "Holonomic and omnidirectional vehicle with conventional tires," Proceedings of the 1996 IEEE International Conference on Robotics and Automation, pp. 3671-3676, 1996.

[19] M. Wada, et al., "Caster drive mechanisms for holonomic and omnidirectional mobile platforms with no over constraint," Proceedings of the International Conference on Robotics and Automation, pp. 1531-1538, 2000.